Adsorption of Glucose Oxidase onto Plasma-Polymerized Film Characterized by Atomic Force Microscopy, Quartz Crystal Microbalance, and Electrochemical Measurement

Hitoshi Muguruma,* Yoshihiro Kase, Naoya Murata, and Kazunari Matsumura

Faculty of Engineering, Shibaura Institute of Technology, 3-7-5 Toyosu, Koto-ku, Tokyo 1358-8548, Japan

Received: June 16, 2006; In Final Form: October 26, 2006

Adsorption of glucose oxidase (GOD) onto plasma-polymerized thin films (PPF) with nanoscale thickness was characterized by atomic force microscopy (AFM), quartz crystal microbalance (QCM), and electrochemical measurements. The PPF surface is very flat (less than 1-nm roughness), and its properties (charge and wettability) can be easily changed while retaining the backbone structure. We focused on three types of surfaces: (1) the pristine surface of hexamethyldisiloxane (HMDS) PPF (hydrophobic and neutral surface), (2) an HMDS PPF surface with nitrogen-plasma treatment (hydrophilic and positive-charged surface), and (3) an HMDS PPF surface treated with oxygen plasma (hydrophilic and negative-charged surface). The AFM image showed that the GOD molecules were densely adsorbed onto surface 2 and that individual GOD molecules could be observed. The longer axis of GOD ellipsoid molecules were aligned parallel to the surface, called the "lying position", because of electrostatic association. On surface 1, clusters of GOD molecules did not completely cover the original PPF surface (surface coverage was ca. 60%). The 10-nm-size step height between the GOD clusters and the PPF surface suggests that the longer axes of individual GOD molecules were aligned perpendicular to the surface, called the "standing position". On surface 3, only a few of the GOD molecules were adsorbed because of electrostatic repulsion. These results indicate that the plasma polymerization process can facilitate enhancement or reduction of protein adsorption. The AFM images show a corresponding tendency with the QCM profiles. The QCM data indicate that the adsorption behavior obeys the Langmuir isotherm equation. The amperometric biosensor characteristics of the GOD-adsorbed PPF on a platinum electrode showed an increment in the current because of enzymatic reaction with glucose addition, indicating that enzyme activity was mostly retained in spite of irreversible adsorption.

1. Introduction

There is great interest in immobilizing proteins selectively on surfaces to develop biosensors, which convert information about a chemical or set of chemicals into an electronic signal using biological substances such as proteins and nucleic acids. Recently, the concept of biosensors has been extended to other applications such as protein microarray chips for proteome analysis,[1−3] capillary electrophoresis chips for protein separation,[4,5] miniature bioreactors,[6,7] biofuel cells,[8,9] and bio-microelectromechanical systems (BioMEMS).[10−12] These novel biosensors are typically fabricated using micromachining or silicon technology processes, such as vacuum evaporation, plasma etching, photolithography, and lift-off. However, the relationship between surface modification and the structure of a protein-adsorbed surface still remains a fundamental problem, since the performance of the biosensors is dominated by the combination technique used to combine these two components.

Relevant research in this area includes surface modification of charge or hydrophilicity, for example, polystylene derivatives,[13,14] self-assembled monolayers (SAMs),[15−19] silica (silanization),[20−22] and polyelectrolyte multilayers (PEMs),[23,24] to enhance or reduce protein adsorption. In addition to control of protein adsorption, orientational control of the proteins is also possible.[15] This technique is often called "protein architecture", wherein the strategy is primarily to address the protein adsorbed onto polymer supports.

* To whom correspondence should be addressed. Tel: +81-3-5859-8320; fax: +81-5859-8201; e-mail: muguruma@sic.shibaura-it.ac.jp.

However, there are problems in most of the above-mentioned strategies including the following. (1) Some modification techniques cannot control the desired properties while still retaining other properties. For example, in the case of SAMs, in addition to surface properties, such as charge and wettability, the membrane structure (e.g., defects) is also changed. (2) In polystyrene derivatives and PEMs, nanoscale control of the membrane thickness and surface roughness is difficult. (3) SAMs, silanization, and PEMs strongly depend on the surface properties of the substrate such as gold, Si−OH, and positive/negative charge. (4) There are few previous reports on comparisons between the surface structure and sensor characteristics. Moreover, from a practical aspect, these techniques also involve a fatal disadvantage, which is that "wet-chemical" base processes are not a friendly platform for the "dry" processes for the new biosensors.

Plasma-polymerized thin films (PPFs), formed in a plasma in the vapor phase, have the potential to be used in interfacial design for biosensor applications.[25] The properties of the PPFs including the following: They (1) are extremely thin ($<1\ \mu$m), (2) provide good adhesion to the substrate, (3) are pinhole free and present a flat surface structure, (4) are mechanically and chemically stable because of the highly branched and cross-linked polymer structure, and (5) allow for a large amount of biological components to be loaded onto the surface of the film. A plasma process with a non-polymerized monomer (e.g., oxygen, nitrogen, and ammonia) is utilized as a surface modification and graft polymerization.

10.1021/jp063755m CCC: $33.50
Published on Web 12/07/2006

For example, PPFs have been utilized as nanocoatings on noble metals (electrodes) for protein immobilization.[25] Applications include enzyme amperomertric biosensors,[26,27] quartz crystal microbalance (QCM) biosensors,[28,29] and surface plasmon resonance biosensors.[30,31] There are also advantages for fabrication strategies such as BioMEMS processes[10,11] and as inside wall coatings for capillary electrophoresis.[32,33] Although for PPFs, the process of adsorbing proteins onto the surface is a critical step in assembling biosensors, direct observations of this process and its relationship to sensor characteristics have not been previously investigated. Therefore, the aim of this research is to focus on such observations to develop a better understanding of the interfacial structure of biofunctional thin films in biosensors. In this work, glucose oxidase (GOD), which is utilized as an amperometric biosensor for diagnostic instruments and for blood sugar control for diabetes, is used as a model protein.

2. Experimental Section

2.1. Chemicals. Distilled water, potassium dihydrogenphosphate, disodium hydrogenphosphate, and D-glucose were purchased from Kanto Chemical Inc. (Tokyo, Japan). Glucose oxidase (GOD) from *Aspergillus niger* (EC 1.1.3.4, type VII-S) was purchased from Sigma (St. Louis, MO). Hexamethyldisiloxane (HMDS) was purchased from Aldrich (Milwaukee, WI). All reagents in this work were used without further purification.

2.2. Procedure for GOD Adsorbed onto PPF. A plasma generator obtained from Ulvac, Inc. (VEP-1000, Tokyo, Japan) was used for the deposition onto a metal electrode or a silicon substrate as a surface for enzyme adsorption. The silicon substrate or thin-film platinum electrodes (for a glucose biosensor) were placed at the center of the plasma reactor and 50 mm above the edge of the plasma gun. The monomer was placed in a bottle reservoir, which was connected to an inlet line through a mass flow controller. The reactor chamber was evacuated to a base pressure below 10^{-3} Pa, and the monomer was then supplied to the chamber. The parameters were set as follows for generating an organic plasma from the HMDS monomer: power, 200 W; pressure, 0.6 Pa; deposition rate, 22.2 $\pm$ 2.8 nm/min; deposition time, 60 s for atomic force microscopy (AFM) and QCM measurements, 5 s for biosensor fabrication. Subsequently, to introduce amino groups (with a positive charge at pH 7), the HMDS PPF surface was treated with a nitrogen plasma with the following parameters: power, 100 W; flow rate, 15 mL min^{-1}; pressure, 3 Pa; exposure time, 20 s. Also, to modify the negative charge (introduction of carboxyl groups), the HMDS PPF surface oxygen plasma was treated with an oxygen plasma under the same conditions as the nitrogen plasma. The procedure for GOD adsorption is as follows. An aliquot of GOD dissolved in the phosphate buffer (pH 7, 20 mM) was dropped onto the film for 1 h. The sample was then washed with distilled water thrice to eliminate the salt from the buffer solution.

2.3. Biosensor Device Fabrication. An electrochemical biosensor device was formed on a 150-μm-thick glass substrate with planar dimensions of approximately 50 $\times$ 50 mm^2. All the metal layers were sputter-deposited and patterned using a mask process. Glass slides used to make thin film electrodes were cleaned in 50% nitric acid for 1 h and then were rinsed with water and acetone. The platinum (Pt) thin films were sputtered using an apparatus manufactured by Ulvac, Inc. (VEP-1000, Tokyo, Japan). Their thicknesses (200 nm) were determined by a surface profiler and a quartz crystal microbalance. A 40-nm-thick chromium (Cr) intermediate layer was used to promote adhesion of the Pt layer. HMDS PPF was deposited onto the Pt electrode, and subsequent nitrogen plasma treatment was carried out if it was necessary. Finally, the GOD solution was dropped onto the PPF surface and was washed by deionized water. The dimensions of the openings of the working electrode were 5 $\times$ 5 mm^2.

2.4. Measurements. Atomic force microscopy (AFM) was carried out in the tapping mode in a normal atmosphere using a commercial AFM system (NanoScope IIIaAFM Dimension 3000 stage system, Nihon Veeco KK, Tokyo, Japan). The scanning tip was equipped with an AC mode supersharp chip purchased from Nanosensors Inc. (Neuchatel, Switzerland). The scanning rate was 0.6 Hz. AFM system software was used to analyze the image data to calculate defined features such as the root-mean-square roughness values (R_{rms}), the arithmetic mean of the departure of the roughness profile from the mean line (R_a), and the maximum z-range values (R_{max}).

Electrochemical measurements were performed using an electrochemical analyzer (ALS Instruments, Model 701A West Lafayette, IN). The three-electrode configuration was used. The reference electrode (Ag/AgCl, RE-1C) and counter electrode (Pt) were purchased from Bioanalytical Systems Inc. The working electrode composed of a PPF biofilm was fabricated. Electrochemical measurements were carried out in a 10-mL vessel at ambient temperature (23 $\pm$ 1 °C). A phosphate buffer (20 mM, pH 7) was used as the supporting electrolyte. To prepare samples at the designated concentrations, a stock solution of glucose (0.1 M or 1 M) was successively added, and the procedure was repeated.

An affinixQ was used as a quartz crystal microbalance (QCM) instrument (Initium Co. Ltd, Tokyo, Japan) with 10-mL cells equipped with an AT-cut 27 MHz QCM plate (8-mm-diameter quartz plate and an area of 4.9 mm^2 of the Au electrode) at the bottom of the cell along with a stirring bar with a temperature control system. The Au electrodes on the QCM were modified by PPF using the conditions described in section 2.2. The QCM Au electrode was coated with PPF and was immersed in a solution (phosphate buffer 20 mM, pH 7, 25 °C). The affinity of GOD was determined from the frequency changes (ΔF) due to changes in mass on the electrode surface. In this experiment, a frequency decrease of 1 Hz corresponded to a mass increase of 0.62 $\pm$ 0.1 ng cm^{-2}.[34]

The zeta (ζ) potentials of the PPF surfaces were measured using an ELS-800 instrument (Otsuka Electronics, Osaka, Japan). The electrophoretic mobility (u) of polystyrene particles at the PPF surfaces was measured, and the mobility obtained was converted into a zeta potential using the Smoluchowski equation, $\zeta = 4\pi\eta u/\epsilon$, where η is the viscosity of the solution and ϵ is the dielectric constant of the solvent.

3. Results and Discussion

3.1. Surface Chemistry of PPF. An AFM image of a pristine PPF, which was observed to be free of pinholes, defects, platelets, granules, terraces, and so forth, has been previously reported.[35] The surface roughness data is shown in Table 1. In plasma polymerization, the structure obtained is not necessarily based upon that of the original monomer since the process occurs via random generation of unstable intermediate species under a high-energy plasma.[36] The HMDS PPF has a variety of three-dimensional cross-linked network conformations with several silicon atoms surrounded by oxygen atoms and methyl groups,[37] creating highly hydrophobic surfaces.[36] The surface roughness-related parameter values (R_{rms} = 0.21−0.35 nm,

TABLE 1: Surface Data of GOD Adsorbed onto Plasma-Polymerized Film

surface (abbreviation in text)	bulk concentration (mg/mL)	AFM image	AFM data (nm) R_{rms}	R_a	R_{max}
HMDS			0.35	0.27	2.6
HMDS−N			0.21	0.24	2.4
HMDS−O			0.26	0.30	2.5
HMDS−GOD	10	Figure 1A	2.8	2.3	14
HMDS−N−GOD	10	Figure 1B	0.73	0.56	6.6
HMDS−O−GOD	10	Figure 1C	0.62	0.39	6.1
HMDS−N−GOD	0.1	Figure 3B	0.55	0.44	3.8
HMDS−N−GOD	0.001	Figure 3C	0.47	0.37	3.5

Table 1) were similar to those of silicon[38] and mica,[39,40] indicating that the PPF has a very flatter surface than other polymer surfaces. This surface roughness was not changed with subsequent plasma treatment (non-polymerized monomer gas of nitrogen and oxygen) for surface modification (Table 1). Because of the small surface roughness (0.35 nm), the surface provides reasonable resolution with sizes of 10 nm or less for AFM measurements.

One of the advantages of plasma polymerization is the simple and easy surface modification. Here, we investigate the adsorption behavior of GOD for three kinds of surfaces obtained by the plasma process. The first is the pristine surface of HMDS PPF, which has a hydrophobic and neutral nature (contact angle with water was more than 90°, see Figure S1A), defined as HMDS. The second is a nitrogen plasma-treated HMDS, with a hydrophilic nature (contact angle with water was less than 50°, see Figure S1B) and positive charge at pH 7 (ζ-potential was ca. 20 mV), defined as HMDS−N. In the presence of the nitrogen plasma, rearrangement reactions may occur such that the nitrogen atoms at the surface form primary amines.[41] The third surface is an oxygen-plasma-treated HMDS, with a hydrophilic nature and negative charge at pH 7 (ζ-potential was ca. −40 mV) because of the introduction of acid functional groups, defined as HMDS−O.[41] The surface concentration for charged groups (amino and carboxyl) was ca. 3×10^{13} cm^{-2} which is the saturation concentration.[29,41]

This indicates that the plasma process is effective for surface control with retention of the bulk structure (e.g., surface roughness and polymer backbone).

3.2. AFM Measurements. First, we are aware that the dimensions of a deglycosylated GOD molecule have been reported to be 6.0 nm × 5.2 nm × 7.7 nm from crystal structure data.[42] Therefore, the actual size of the native GOD should be somewhat larger. The macroscopic shape of the GOD molecule is ellipsoid with a long axis of 10−14 nm and a short axis of 6−8 nm. Figure 1 shows AFM images of adsorbed GOD on the three types of PPF surfaces.

On HMDS−GOD, the original surface of the PPF was incompletely covered by the GOD clusters (Figures 1A and S2−4). The coverage of the adsorbed GOD layer region was 60%. The surface domain with no adsorption was the pristine HMDS surface because its surface roughness value was similar to that of the pristine HMDS. The step height between the adsorbed GOD clusters and original surface of PPF was 8.9 ± 0.2 nm (cross-sectional profile in Figure 1A), and the maximum step height was 14 nm. This value was close to the long axis of the GOD molecule, indicating that a molecule of GOD tends to position itself with its longer axis aligned perpendicular to the surface (standing position, see lower inset of Figure 2A). The protein cluster did not grow vertical to the substrate but rather grew along the in-plane direction. The driving force for this could be the van der Waals force of the clusters and the physical force between the hydrophobic domain of GOD and the surface.

On HMDS−N−GOD, the protein layer formed by the adsorbed-GOD array is observed (Figures 1B, S5, and S6). The surface flatness of pristine HMDS PPF enhanced the AFM resolution, enabling imaging of a single enzyme molecule: the imaged ellipsoids were usually identified as two-dimensional objects (12.2 ± 1.2 nm × 8.3 ± 0.9 nm; arrows in Figure 1B) and had a step height of 2.7 ± 0.2 nm. This value was smaller than the minimum dimension (short axis) of the GOD molecules since the object was the densely packed GOD array. Instead, a maximum step height of R_{max} = 6.6 nm could represent the thickness of the protein layers since R_{max} probably corresponds to the height between the defect (pristine surface) and the top of the adsorbed GOD. The observation of the structure of adsorbed-GOD is similar to the data measured using ellipsometry[43] and scanning tunneling microscopy.[44] The object size in our identification strongly indicates that the ellipsoid shown in Figure 1B must be a visualized image of a single molecule of GOD with its longer axis aligned parallel to the surface (lying position, see lower inset of Figure 1B).[43] The difference in orientation between HMDS−GOD and HMDS−N−GOD is also supported by the fact that the surface roughness (R_{rms} and R_a, Table 1) for HMDS−GOD is much larger than for HMDS−N−GOD.

There were no observations of larger sizes of the clusters, higher vertical steps than the size of single protein molecules, or defects in the adsorbed protein. This suggests that the protein layer is a two-dimensional, densely packed array and that the adsorption obeys the Langmuir isotherm (see discussion in section 3.3). This is because the electrostatic interaction play an important role as the driving force for adsorption; the affinity between the negatively charged GOD (pI = 4.2) and the positively charged surface[45] is larger than the aggregation forces among the GOD molecules, despite the high bulk concentration (10 mg/mL) of the enzyme solution used. In contrast, previous reports of AFM images of GOD adsorbed onto gold showed isolated single molecules[46] or clusters of several GOD molecules.[47−49] The finding result that the HMDS−N surface has higher affinity than the other surfaces is indeed remarkable.

On HMDS−O−GOD, the AFM image shows the original PPF surface and only several single molecules of adsorbed-GOD (Figure 1C). The step height (4.2 ± 0.2 nm) due to isolated GOD is close to the thickness of a densely packed array of GOD, as in Figure 1B. This is supported by the fact that the R_{max} values of HMDS−N−GOD (R_{max} = 6.6 nm) and HMDS−O−GOD (R_{max} = 6.1 nm) were very similar. Therefore, the GOD molecules are also in a lying position similar to the case of HMDS−N−GOD (Figure 1B). The value of R_{rms}(R_a) = 0.62 (0.39) nm for HMDS−O−GOD is slightly smaller than the R_{rms}-(R_a) = 0.73 (0.56) nm for HMDS−N−GOD (Table 1). This is because the surface roughness indicates the average profile for all regions of the surface, and thus, the amount of adsorbed GOD in HMDS−O−GOD is much smaller than in HMDS−N−GOD. The protein-resistant effect is similar to that observed

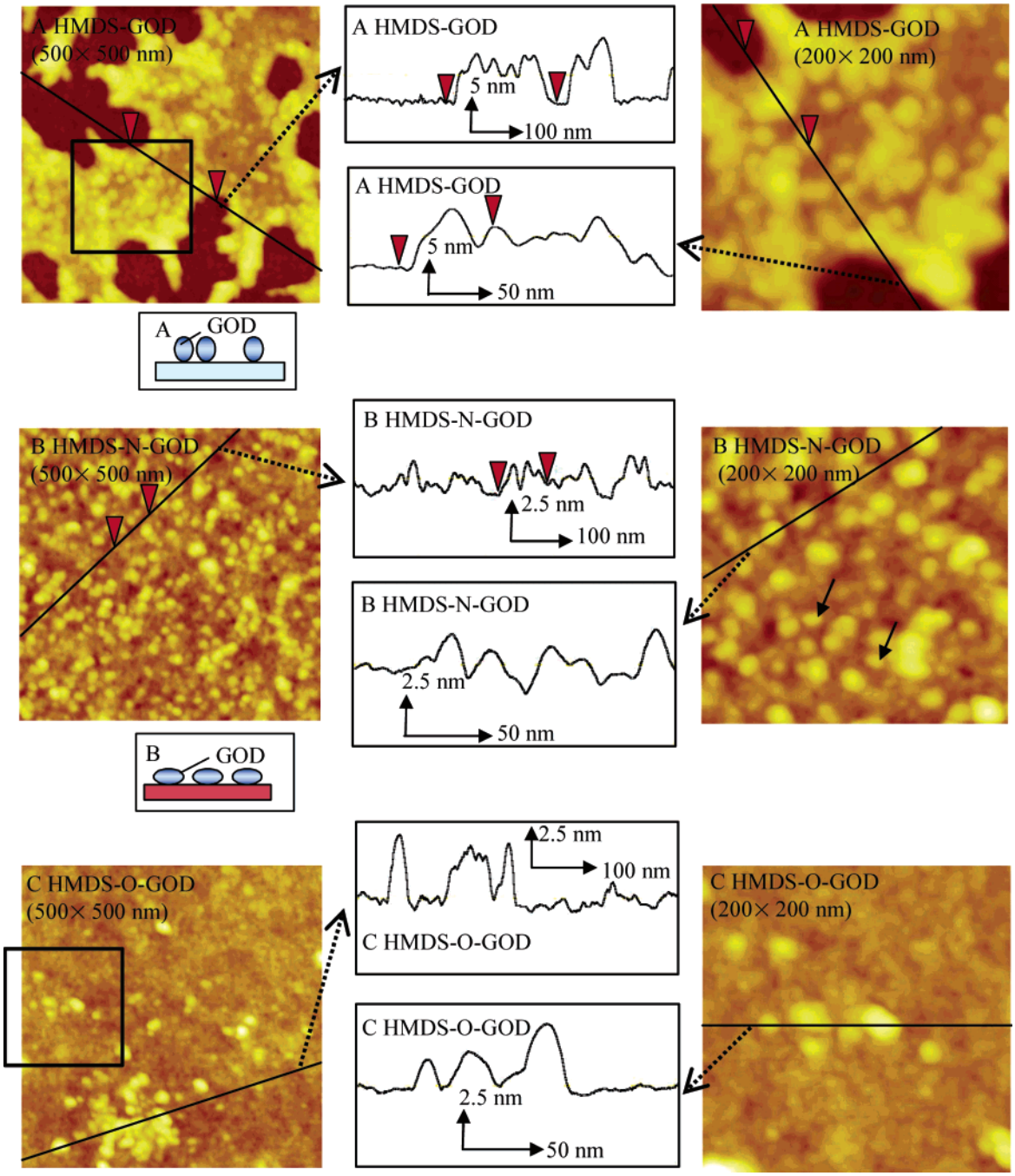

Figure 1. Tapping-mode AFM images and cross-sectional surface profiles of plasma-polymerized films (PPFs) after adsorption of GOD onto an HMDS PPF surface. (A) Pristine HMDS PPF (HMDS−GOD); (B) HMDS PPF treated with nitrogen plasma (HMDS−N−GOD); (C) HMDS PPF treated with oxygen plasma (HMDS−O−GOD). The bulk concentration of GOD was 10 mg/mL. The squares in the 500-nm scale image of A and C correspond to the enlarged 200-nm scale image views shown on the right. The arrows in B represent a single molecule of GOD. The red triangles in A and B correspond to those in the cross-sectional profiles. Image size: 200 and 500 nm. *z*-scale (contrast): (A) 20, (B, C) 10 nm; scan rate: 0.6 Hz. The lower insets in A and B are schematic illustrations of the enzyme orientation on the surface. Surface data are shown in Table 1.

in polyethylene glycol (PEG)-like surfaces in which PEG chain mobility causes their protein-resistant behavior in antifouling processes.[50,51] However, the mechanism here is different. In our case, oxygen plasma treatment introduces carboxyl groups and yields a negative charge at pH 7. The electrostatic repulsion by the negative charge as well as the small actual surface area (very flat surfaces) reduces the interaction between the GOD molecule and the surface of HMDS−O.

3.3. QCM Measurements. Quartz crystal microbalance (QCM) measurements allow for direct assessment of the time-dependent adsorption process. The PPFs are suitable for coating on the QCM electrode because of their nanoscale thickness, flatness, strong adhesion, and homogeneous nature.[29] Although the QCM results represent the adsorption behavior of proteins, they cannot provide any orientation information. Instead, the "dynamic" information for protein adsorption can be obtained by QCM that cannot be obtained by AFM: AFM only provides the image profile as "static" information. Figure 2 show the time−frequency profiles for GOD adsorption onto the various PPF surfaces.

Adsorption data at 0.1 mg/mL of the GOD concentration onto the three surfaces showed that the time to reach steady-state adsorption and the frequency change when the time reaches a steady-state adsorption varied with the surface properties. The

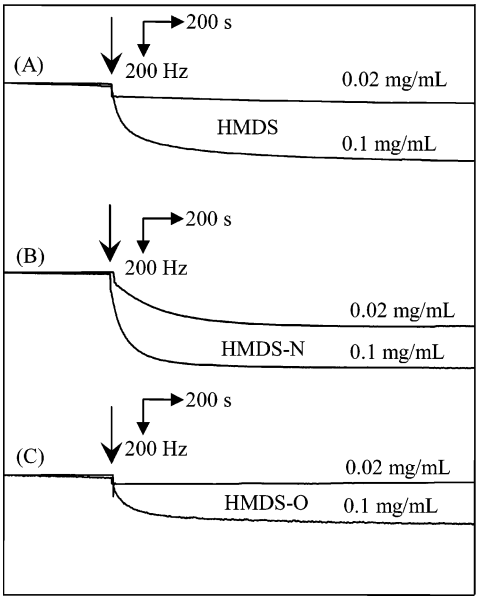

Figure 2. Resonant frequency response in 20 mM phosphate buffer (pH 7.0) at 25 °C. The quartz crystal microbalance was coated with (A) pristine HMDS PPF (HMDS), (B) HMDS PPF treated with nitrogen plasma (HMDS−N−GOD), and (C) HMDS PPF treated with oxygen plasma (HMDS−O−GOD). Arrows indicate the addition of 0.02 mg/mL or 0.1 mg/mL GOD solution.

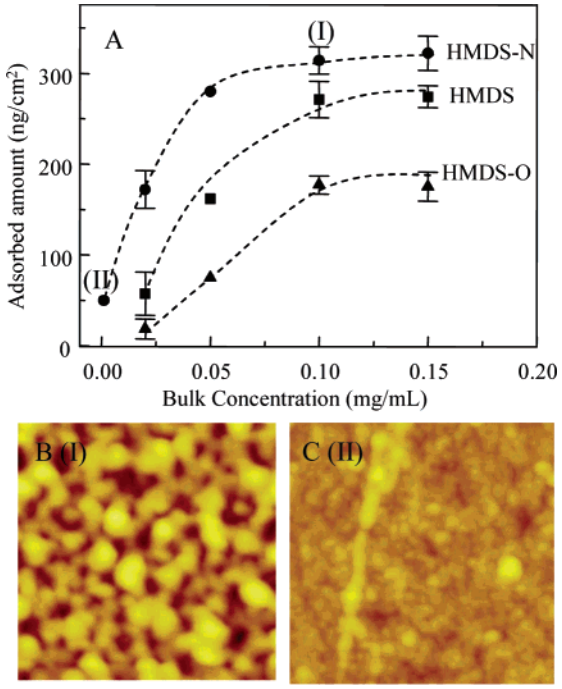

Figure 3. (A) Adsorption isotherms of GOD on pristine HMDS PPF, HMDS PPF treated with the nitrogen plasma, and HMDS PPF treated with the oxygen plasma. Experiments were performed in 20 mM pH 7 solution at 25 °C. Surface concentrations (Γ) were determined after 60 min for the adsorption time. (B, C) Tapping-mode AFM images of plasma-polymerized films (PPFs) after GOD was physisorbed onto the HMDS PPF treated with the nitrogen plasma. The GOD bulk concentrations were (B) 0.1 mg/mL (HMDS−N−GOD, corresponding to (I) in the adsorption isotherms of Figure 3A) and (C) 0.001 mg/mL (HMDS−N−GOD, corresponding to (II) in the adsorption isotherms of Figure 3A). Image size: 200 nm; *z*-scale (contrast): 10 nm; scan rate: 0.6 Hz. Surface data are shown in Table 1.

higher the interaction between GOD and the surface, the larger was the saturated amount of adsorption and the saturation adsorption was reached faster. The frequency change (ΔF) of 507 Hz corresponds to 314 ± 50 ng/cm^2 of GOD, according to Sauerbrey's equation.[52] The 314 ± 50 ng/cm^2 of adsorbed amount in HMDS−N−GOD (Figure 2B) is close to the maximum for two-dimensional dense arrays observed by AFM (Figure 1B). The highest surface concentration of GOD was estimated to be 1.6×10^{-12} mol/cm^2, on the basis of the assumption that the enzyme is a compact ellipsoid with approximate dimensions of 12.2×8.3 nm^2 (as measured by AFM), and forms a densely packed monolayer. Then, since GOD is a dimeric protein with a molecular weight of 160 kDa, the highest surface concentration is estimated to be 300−400 ng/cm^2. Therefore, GOD is densely adsorbed onto HMDS−N−GOD with 0.1 mg/mL bulk concentration.

In contrast, the 280 ng/cm^2 adsorbed amount in HMDS−GOD obtained by QCM (Figure 2A) is larger than that observed by AFM when the surface coverage of GOD layer was ca. 60% (Figure 1A). The 172 ng/cm^2 adsorbed amount in HMDS−GOD (Figure 2C) is detected by QCM in spite of the fact that few GOD molecules are adsorbed according to AFM observations (Figure 1C). In other words, there is a tendency for the amount of adsorbed-GOD evaluated by QCM to be larger than that obtained by AFM. This inconsistency is probably because weakly adsorbed GOD was washed out in the AFM samples. The adsorbed GOD in the AFM image thus shows irreversible adsorption. In general, there is a tendency for the conformation of a strongly adsorbed protein to change.[13] However, this is not applicable in our case (see discussion in section 3.4).

QCM can evaluate the dynamic information for protein adsorption by the frequency changes (ΔF) that can be fit to the equation, $\Delta F = A \exp(-kt)$, where k is a rate constant. The time to reach steady-state adsorption shows a similar tendency; the time in HMDS−N is ca. 500 s ($k = 0.9-1.2 \times 10^{-2}$ s^{-1}), whereas the time in HMDS and HMDS−O is more than 2500 s ($k = 3.2 \times 10^{-3}$ s^{-1}). The noise level of the baseline in HMDS−O is larger than that in HMDS−N, indicating that GOD molecules were adsorbed and desorbed at the surfaces because of weak interaction.

The adsorption behavior for 0.02 mg/mL GOD concentration shows a similar tendency as the behavior at 0.1 mg/mL. In HMDS−N, the time to reach saturation (ca. 2000 s, $k = 4.0 \times 10^{-3}$ s^{-1}) at 0.02 mg/mL is 4 times larger than that at 0.1 mg/mL of the GOD bulk concentration. On the other hand, there is a distinct difference in the saturated adsorption amount (Γ_{sat}); Γ_{sat} in HMDS−N−GOD is much larger than that in HMDS−GOD and HMDS−O−GOD, showing the affinity between GOD molecules and PPF surfaces.

Figure 3A shows the adsorbed amount of GOD as a function of the GOD concentration in the solution. The adsorption time of 1 h in this experiment is probably sufficient for achieving saturated adsorption. This indicates that the adsorption follows the Langmuir isotherm. Adsorption for other proteins onto polymer surfaces also obeys this law.[21,22,53] The bulk concentration for reaching saturation is around 0.1 mg/mL.

Figure 3B and C shows tapping-mode AFM images of plasma-polymerized films (PPFs) after GOD was physisorbed onto HMDS PPF treated with nitrogen plasma to investigate the dependence of the enzyme density on the original concentration in the adsorbate solution. The fact that the surface image of HMDS−N−GOD in 0.1 mg/mL (Figure 3B) resembles that in 10 mg/mL (Figure 1B) follows the Langmuir isotherm with no multilayer adsorption. However, the surface roughness of HMDS−N−GOD for 0.1 mg/mL concentration is slightly smaller than that for a 10 mg/mL concentration (Table 1), suggesting that the amount of adsorbed GOD for HMDS−N−

GOD in the case of the 0.1 mg/mL concentration is slightly smaller than that for the 10 mg/mL concentration.

On the surface wherein the adsorption process was carried out with 0.001 mg/mL of bulk GOD concentration, GOD is not observed (Figure 3C). The surface image is similar to that of the pristine HMDS PPF surface, that is, the surface roughness and cross-sectional profiles are very similar to each other.[35] However, the surface roughness (R_a = 0.37 nm) of HMDS−N−GOD for the 0.1 mg/mL concentration is similar to that in HMDS−O−GOD (R_a = 0.39 nm) from Table 1, suggesting that there are a few GOD molecules on the surface. It is concluded that the surface image in Figure 3 shows a corresponding tendency with the QCM profiles. Unfortunately, we could not investigate QCM data for the 10 mg/mL of bulk solution case because it was difficult to eliminate the signal due to high viscosity.

The above results of AFM imaging and QCM measurements show that plasma treatment is effective in altering surface properties for the control of protein attachment (enhancement or reduction) or orientation (lying or standing position). The positively charged surface nitrogen plasma treatment shows good affinity with the negatively charged proteins. Therefore, this provides an ideal protein-terminated surface for biosensor applications.

3.4. Enzyme Biosensor Characteristics. The most important feature for biosensor applications is maintaining the tertiary structure of proteins. In the case of biosensors, this affects biosensor characteristics such as sensitivity, selectivity, and long-term-stability. GOD is the most popular protein for enzymatic biosensors. The relationship between the enzyme biosensor characteristics and protein−PPF structure was investigated. Electrochemical measurements were conducted in the present study, and the main purpose for these measurements was to obtain information on enzymatic activity, which cannot be investigated using AFM and QCM. A device wherein the protein immobilized HMDS−GOD and HMDS−N−GOD onto the sputtered platinum electrode was fabricated. To show evidence of the amperometric system because of the enzymatic reaction, a cyclic voltammogram (CV) is appropriate and can be used. Figure 4A and B shows cyclic voltammograms of the device (enzyme-immobilized working electrode) and the glucose response. The sensor response is due to the following enzymatic reaction:

$$\beta\text{-D-glucose} + O_2 \rightarrow \beta\text{-gluconolactone} + H_2O_2 \quad (1)$$

The hydrogen peroxide generated in this reaction passes through the PPF (2-nm thickness in this experiment) between the GOD and the electrode and reaches the electrode because the mesh size of HMDS PPF is larger than that of hydrogen peroxide.[26] Subsequently, this is electrochemically reduced at the Pt anode. The electrode is polarized to more than +600 mV versus the Ag/AgCl reference electrode. This reaction is represented by the following equation:

$$H_2O_2 \rightarrow 2H^+ + O_2 + 2e^- \quad (2)$$

The catalytic ability of the Pt electrode is sensitive to the roughness of the surface.[54] The sputtered Pt electrodes used in the present study were obtained from the same batch to obtain reproducibility of sensor response. Figure 4A and B shows CVs in glucose solutions of various concentrations using devices with HMDS−GOD and HMDS−N−GOD biothin films, respectively. In the absence of glucose, the enzymatic reaction did not proceed and no hydrogen peroxide was produced. Thus, nothing but a small oxidation current appeared in all the devices. In the presence of glucose, the oxidation current of hydrogen peroxide appeared at over +300 mV and peaked at +600 mV owing to the enzymatic production of hydrogen peroxide, indicating that enzyme activity was almost retained (i.e., no conformational change) in spite of irreversible adsorption. Figure 4C shows the calibration plot for glucose on the basis of the current response of CVs. The current increased with glucose concentration. The results indicate that the sensor response covers use for diabetes (ca. 5−20 mM).

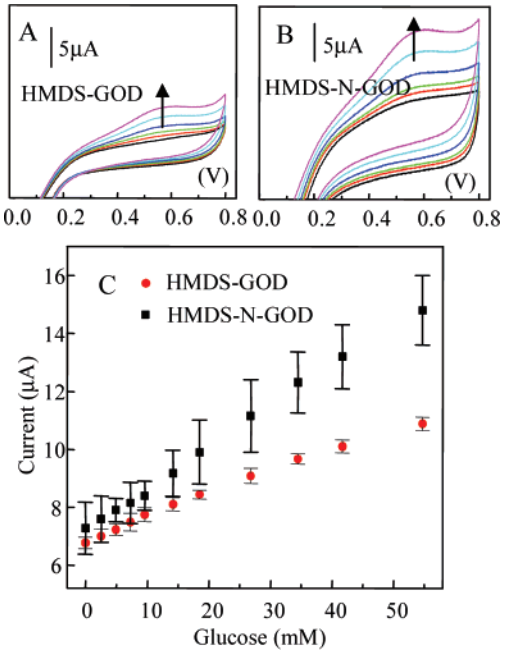

Figure 4. Cyclic voltammograms of glucose response in which the device is the surface of (A) HMDS−GOD and (B) HMDS−N−GOD on the Pt electrode. The sweep rate was 50 mV s^{-1}. The glucose concentration is 0, 4.9, 9.6, 18.5, 34.5, and 54.7 mM in the arrow direction. (C) Calibration curve based on the oxidation current at +600 mV under cyclic voltammograms. Circle: HMDS−GOD, sensitivity, 76.6 nA cm^{-2} mM^{-1}, linear range (r > 0.97), 0−18.5 mM; triangles: HMDS−N−GOD, sensitivity, 146 nA cm^{-2} mM^{-1}, linear range (r > 0.97), 0−26.8 mM.

The sensitivity of HMDS−N−GOD (146 nA mM^{-1}) is 2 times larger than that of HMDS−GOD (76.6 nA mM^{-1}). This difference is probably due to the amount of immobilized enzyme, that is, the sensor response did not depend on the molecular orientation but depended only on the amount of immobilized enzyme. This is because there is no steric hindrance for diffusion (access) of a small substrate molecule such as glucose. Szucs et al.[43] reported that the enzyme adsorbed onto the gold electrode gradually unfolds, leading to a significant lowering in enzymatic activity. In our case, the sensor response was maintained during long-term usage (at least 30 repetitions of a CV scan) and a 1 h period of thermal stress at 60 °C (Figure S7). There are two possible reasons for this. One is that the unfolding process of proteins requires space. Since this space is occupied by previously adsorbed molecules in the densely packed array of molecules in our case, the unfolding is blocked.[21] The other reason is that GOD adsorbed onto a charged surface is more stable than that adsorbed onto a gold surface. This is supported by the fact that a cationic polyelectrolyte stabilizes the tertiary structure of protein.[55,56]

4. Conclusions

The adsorption of glucose oxidase (GOD) onto plasma-polymerized films (PPF) was investigated by AFM, QCM, and electrochemical measurements. The GOD molecules were densely adsorbed onto the surface of hexamethyldisiloxane (HMDS) PPF, with subsequent treatment with nitrogen plasma with hydrophilic and positive charge. AFM images showed that the individual GOD molecules on the positively charged PPF surface had their longer axis aligned parallel to the surface, in the so-called lying position, because of electrostatic association. On the hydrophobic PPF (pristine PPF) surface, the AFM image showed that the original surface of the PPF was incompletely covered by the GOD clusters with 60% coverage of the adsorbed GOD layer region. A molecule of GOD tends to position itself with its longer axis aligned perpendicular to the surface in the so-called standing position. On the negatively charged PPF surface, there were few GOD molecules. The results of surface characterization before and after enzyme immobilization showed that this method provides control over the spatial orientation of single enzyme molecules in favor of efficient and reproducible signal generation. The protein layer did not grow toward the vertical to the substrate but rather grew toward the in-plane direction, indicating that the adsorption behavior obeys the Langmuir isotherm. The amperometric biosensor characteristics of the GOD-adsorbed PPF on a platinum electrode showed current increment because of enzymatic reaction with glucose addition, indicating that enzyme activity was retained. The biosensor measurement indicated that the amount of immobilized enzyme is a more important factor than molecular orientation because of the small substrate (glucose). The three kinds of surfaces presented in this article involve distinctive and controllable parameters, therefore, the result provides general information and will be easily expanded. These results are also helpful for a better understanding of the protein architecture for biosensor design. More controlled study, for example, the relation between other parameters of surfaces and orientation of other proteins, is the next stage.

Supporting Information Available: Pure water wettable behavior of HMDS PPF surfaces before and after treatment of nitrogen plasma. More detailed AFM images (HMDS−GOD and HMDS−N−GOD). Data for thermal stability of GOD adsorbed onto PPF. These materials are available free of charge via the Internet at http://pubs.acs.org.

References and Notes

(1) Sage, L. *Anal. Chem.* **2004**, *76*, 137A−142A.
(2) Oleinikov, A. V.; Gray, M. D.; Zhao, J.; Montgomery, D. D.; Ghindilis, A. L.; Dill, K. *J. Proteome Res.* **2003**, *2*, 313−319.
(3) Dayal, B.; Ertel, N. H. *J. Proteome Res.* **2002**, *1*, 375−380.
(4) Xiao, D.; Le, T. V.; Wirth, M. J. *Anal. Chem.* **2004**, *76*, 2055−2061.
(5) Li, Y.; Buch, J. S.; Rosenberger, F.; DeVoe, D. L.; Lee, C. S. *Anal. Chem.* **2004**, *76*, 742−748.
(6) Vilker, T.; Janasek, D.; Manz, A. *Anal. Chem.* **2004**, *76*, 3373−3386.
(7) Dittrich, P. S.; Tachikawa, K.; Manz, A. *Anal. Chem.* **2006**, *78*, 3887−3908.
(8) Barton, S. C.; Gallaway, J.; Atanassov, P. *Chem. Rev.* **2004**, *104*, 4867−4886.
(9) Mano, N.; Mao, F.; Heller, A. *J. Am. Chem. Soc.* **2003**, *125*, 6588−6594.
(10) Hiratsuka, A.; Muguruma, H.; Lee, K.; Karube, I. *Biosens. Bioelectron.* **2004**, *19*, 1667−1672.
(11) Bouaidat, S.; Winther-Jensen, B.; Christensen, S. F.; Jonsmann, J. *Sens. Actuators, A* **2004**, *110*, 391−394.
(12) Gourley, P. L. *Biotechnol. Prog.* **2005**, *21*, 2−10.
(13) Haynes, C. C.; Norde, W. *J. Colloid Interface Sci.* **1995**, *169*, 313−328.
(14) Suzawa, T.; Shirahama, H. *Adv. Colloid Interface Sci.* **1991**, *35*, 139−172.
(15) Chen, S.; Liu, L.; Zhou, J.; Jiang, S. *Langmuir* **2003**, *19*, 2859−2864.
(16) Li, L.; Chen, S.; Jiang, S. *Langmuir* **2003**, *19*, 2974−2982.
(17) Zhou, D.; Wang, X.; Birch, L.; Rayment, T.; Abell, C. *Langmuir* **2003**, *19*, 10557−10562.
(18) Li, L.; Chen, S. Zheng, J.; Ratner, B. D.; Jiang, S. *J. Phys. Chem. B* **2005**, *109*, 2934−2941.
(19) Veiseh, M.; Zareie, M. H.; Zhang, M. *Langmuir* **2002**, *18*, 6671−6678.
(20) Heyes, C. D.; Kobitski, A. Y.; Amirgoulova, E. V.; Nienhaus, G. U. *J. Phys. Chem. B* **2004**, *108*, 13387−13394.
(21) Pancera, S. M.; Alvarez, E. B.; Politi, M. J.; Schimmel, Th.; Petri, D. F. S. *Langmuir* **2002**, *18*, 3517−3523.
(22) Xu, H.; Lu, J. R.; Williams, D. E. *J. Phys. Chem. B* **2006**, *110*, 1907−1914.
(23) Shi, L.; Lu, Y.; Sun, J.; Zhang, J.; Sun, C.; Liu, J.; Shen, J. *Biomacromolecules* **2003**, *4*, 1161−1167.
(24) Salloum, D. S.; Schlenoff, J. B. *Biomacromolecules* **2004**, *5*, 1089−1096.
(25) Muguruma, H.; Karube, I. *TrAC, Trends Anal. Chem.* **1999**, *18*, 62−68.
(26) Muguruma, H.; Hiratsuka, A.; Karube, I. *Anal. Chem.* **2000**, *72*, 2671−2675.
(27) Kase, Y.; Muguruma, H. *Anal. Sci.* **2004**, *20*, 1143−1146.
(28) Wang, H.; Li, D.; Wu, Z.; Shen, G.; Yu, R. *Talanta* **2004**, *62*, 201−208.
(29) Nakanishi, K.; Muguruma, H.; Karube, I. *Anal. Chem.* **1996**, *68*, 1695−1700.
(30) Zhang, Z.; Menges, B.; Timmons, R. B.; Knoll, W.; Förch, R. *Langmuir* **2003**, *19*, 4765−4770.
(31) Nakamura, R.; Muguruma, H.; Ikebukuro, K.; Sasaki, S.; Nagata, R.; Karube, I.; Pedersen, H. *Anal. Chem.* **1997**, *69*, 4649−4652.
(32) Tsai, S.−W.; Loughran, M.; Hiratsuka, A.; Yano, K.; Karube, I. *Analyst* **2003**, *128*, 237−242.
(33) Loughran, M.; Tsai, S.−W.; Yokoyama, K.; Karube, I. *Curr. Appl. Phys.* **2003**, *3*, 495−499.
(34) Nishino, H.; Murakawa, A.; Mori, T.; Okahata, Y. *J. Am. Chem. Soc.* **2004**, *126*, 14752−14757.
(35) Muguruma, H.; Kase, Y.; Uehara, H. *Anal. Chem.* **2005**, *77*, 6557−6562.
(36) Tajima, I.; Yamamoto, M. *J. Polym. Sci., Polym. Chem. Ed.* **1985**, *23*, 615−622.
(37) Krishnamurthy, V.; Kamel, I. L.; Wei, Y. *J. Appl. Polym. Sci.* **1989**, *38*, 605−618.
(38) Senda, K.; Vinogradov, G. K.; Gorwadkar, S.; Morita, S. *J. Appl. Phys.* **1993**, *74*, 6425−6426.
(39) Li, G.; Tobin, J. A.; Denton, D. D. *Appl. Phys. Lett.* **1994**, *64*, 560−562.
(40) Sato, D.; Suwa, T.; Kakimoto, M.; Imai, Y. *J. Photopolym. Sci. Technol.* **1997**, *10*, 149−150.
(41) Everhart, D. S.; Reilley, C. N. *Anal. Chem.* **1981**, *53*, 665−676.
(42) Hecht, H. J.; Kalisz, H. M.; Hendle, J.; Schmid, R. D.; Schomburg, D. *J. Mol. Biol.* **1993**, *229*, 153−172.
(43) Szucs, A.; Hitchens, G. D.; Bockris, J. O. *J. Electrochem. Soc.* **1989**, *136*, 3748−3755.
(44) Losic, D.; Shapter, J. G.; Gooding, J. J. *Langmuir* **2002**, *18*, 5422−5428.
(45) Calvo, E. J.; Etchenique, R.; Pietrasanta, Wolosiuk, A. *Anal. Chem.* **2001**, *73*, 1161−1168.
(46) Otsuka, I.; Yaoita, M.; Higano, M.; Nagashima, S.; Kataoka, R. *Appl. Surf. Sci.* **2004**, *235*, 188−196.
(47) Losic, D.; Gooding, J. J.; Shapter, J. G.; Hibbert, D. B.; Short, K. *Electroanalysis* **2001**, *13*, 1385−1393.
(48) Quinto, M.; Ciancio, A.; Zambonin, P. G. *J. Electroanal. Chem.* **1998**, *448*, 51−59.
(49) Zhang, P.; Tam, W. *Fresenius' J. Anal. Chem.* **2001**, *369*, 302−307.
(50) Mar, M. N.; Ratner, B. D.; Yee, S. S. *Sens. Actuators, B* **1999**, *54*, 125−1331.
(51) Sharma, S.; Johnson, R. W.; Desai, T. A. *Langmuir* **2004**, *20*, 348−356.
(52) O'Sullivan, C. K.; Guilbault, G. G. *Biosens. Bioelectron.* **1999**, *14*, 663−670.
(53) Kurosawa, S.; Kamo, N.; Arimura, T.; Sekiya, A.; Muratsugu, M. *Jpn. J. Appl. Phys.* **1995**, *34*, 3925−3929.
(54) Gooding, J. J.; Praig, V. G.; Hall, E. A. H. *Anal. Chem.* **1998**, *70*, 2396−2402.
(55) Appleton, B.; Gibsona, T. D.; Woodward, J. R. *Sens. Actuators, B* **1997**, *43*, 65−69.
(56) Lawrence, N. S.; Deo, R. P.; Wang, J. *Anal. Chem.* **2004**, *76*, 3735−3739.